LITHOFLEX WORKSHOP
24-25 JUNE 2008
Research Centre Rotvoll – Trondheim – Norway

Lithoflex theoretical background: Part II: Density-depth functions

Jörg Ebbing
Geological Survey of Norway
NTNU Trondheim

with help of:
Carla Braitenberg Christine Fichler, Laura Marello, Patrizia Mariani, Stephanie C. Werner, Susann Wienecke

StatoilHydro

NGU

150

Density-depth functions

- Densities
- Velocity-density relations
- Density-depth functions
  - in general
  - for sediments
- Compaction models

Densities - Introduction

The gravity signal is an effect of the geometry and density distribution of sources

The density contrast between geological structures governs the size and shape of anomalies

Absolute densities give the level of the observed anomalies
=> importance for crustal thickness estimates

Superposition of sources and ambiguity

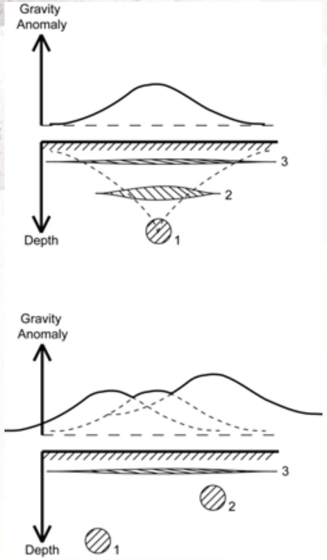

The observed gravity signal is an effect of the superposition sources and different scenarios can produce the same gravity signal: **Ambiguity**

Relative vs. absolute densities

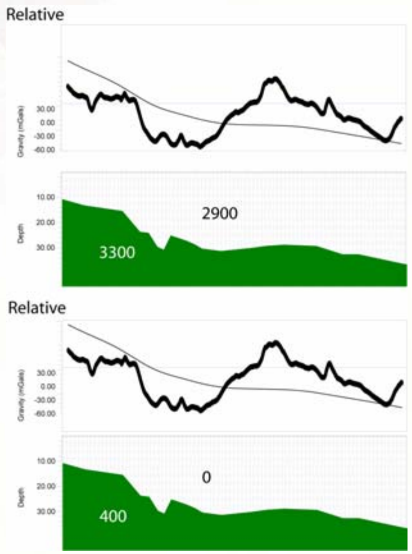

Why do the calculated gravity effects look the same?

Relative vs. absolute densities

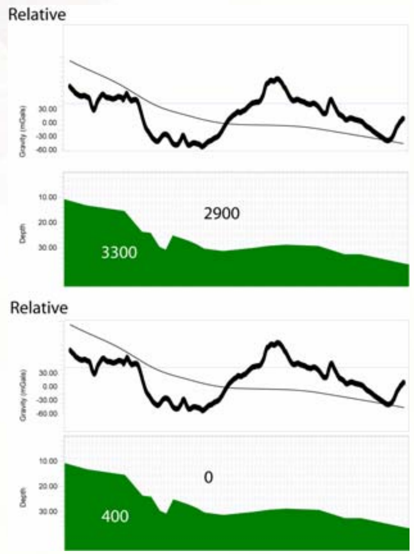

Absolute modelling requires choice of a reference model, e.g. PREM, Crust2.0

How would anomalies look like if we modelled absolute without a reference model?

Relative vs. absolute densities

Absolute modelling requires choice of a reference model, e.g. PREM, Crust2.0

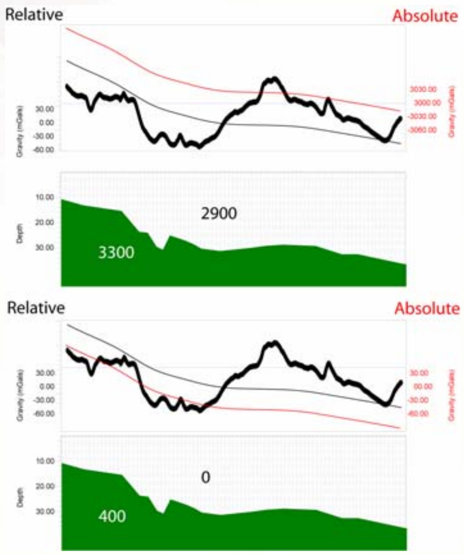

Density distribution in the Earth

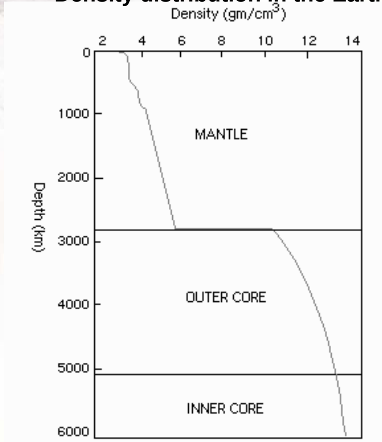

http://www.geologyrocks.co.uk/

Important for normal gravity and planetology, but of less importance for most geological applications

Continental lithosphere densities

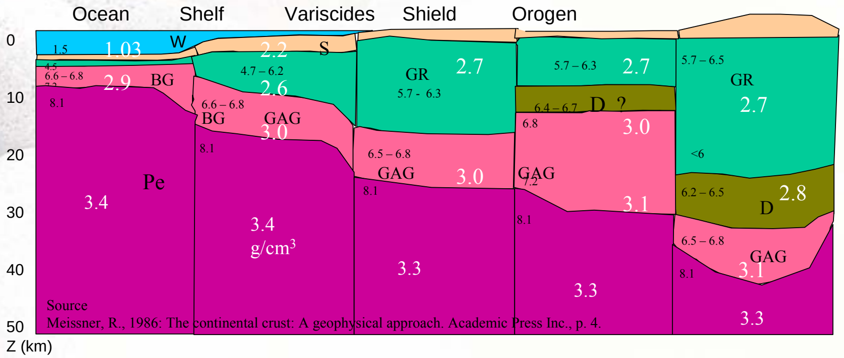

Rock types:

BG = basaltic, gabbroic in oceanic crust
GAG = amphibolitic & granulitic in continental crust
PE = peridotitic, ultramafic
D = Dioritic (?), possibly amphibolitic
S = sediments
GR = granitc gneissic upper crust
W = water

P-wave velocities (km/s):
black numbers

Densities (g/cm^3):
White numbers

Densities can be

- measured from petrophysical samples
- surface sampling, bore-hole logs
- petrophysical experiments
- converted from seismic velocities
- estimated from compaction models

Basic equation: $\rho = \sum_{i=1}^{N} \rho_i \frac{\Delta V_i}{V}$

Densities can be estimated by petrophysical measurement (in the lab) or calculated from seismic velocities using P- and S- velocity to constrain density and material properties

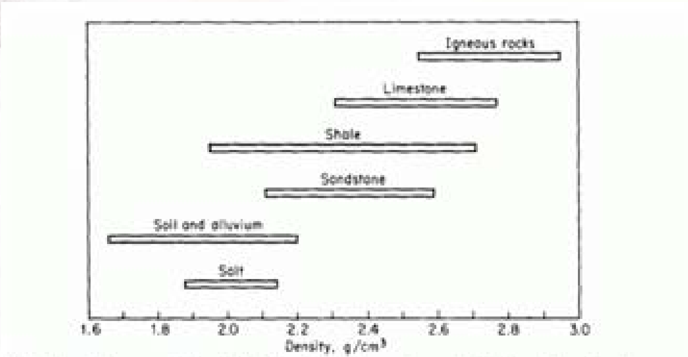

Fig. 7-6 80 percent fiducial limits of small-specimen bulk densities of various kinds of rocks. [From Birch (4).]

CARMICHAEL'S DATABASE, 1984

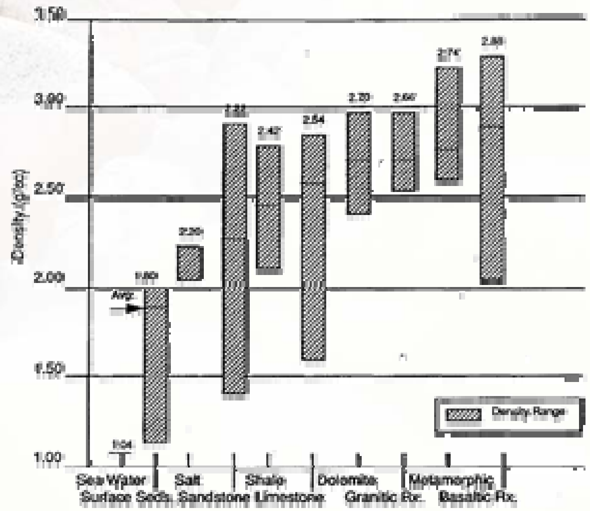

Table 8.1 Densities of some rock types

	Density (Mg/m³)
Unconsolidated	
clay	1.5–2.6*
sand, dry	1.4–1.65
sand, saturated	1.9–2.1
Sediments	
chalk	1.9–2.5
coal, anthracite	1.3–1.8
coal, lignite	1.1–1.5
dolomite	2.3–2.9
limestone	2.0–2.7
salt	2.1–2.6
sandstone	2.0–2.6
shale	2.0–2.7
Igneous and metamorphic	
andesite	2.4–2.8
basalt	2.7–3.0
gneiss	2.6–3.0
granite	2.5–2.8
peridotite	2.8–3.2
quarzite	2.6–2.7
slate	2.6–2.8
Minerals and ores	
barite	4.3–4.7
chalcopyrite	4.1–4.3
galena	7.4–7.6
haematite ore	4.9–5.3
magnetite ore	4.9–5.3
pyrite	4.9–5.2
sphalerite	3.5–4.0
Other	
oil	0.6–0.9
water	1.0–1.05

*The ranges of values (taken from a variety of sources) are approximate. Densities depend partly on whether the rock is weathered and the degree of its porosity.

Source:
Mussett, A. E., Khan, M.A., 2000. Looking into the earth. An introduction to Geological Geophysics. Cambridge University Press

Surface densities

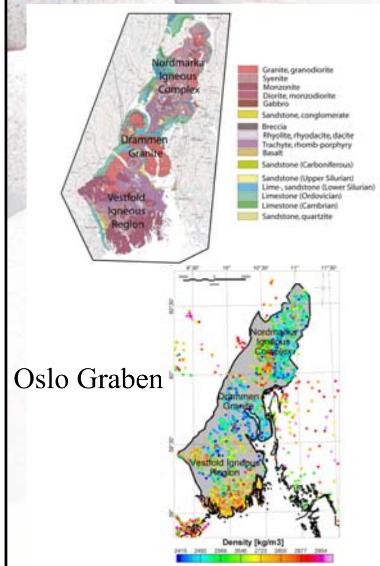

Oslo Graben

Ebbing et al. 2007

Austria

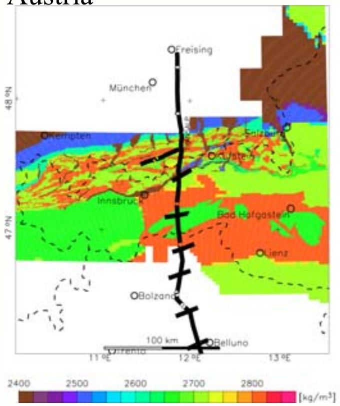

Ebbing 2002

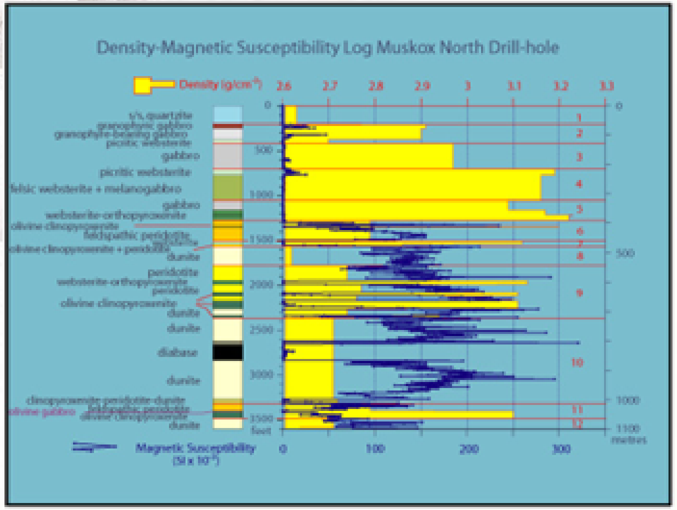

http://ess.nrcan.gc.ca/2002_2006/nrd/slavecomp/muskox_poster_e.php

Mantle densities from laboratory experiments

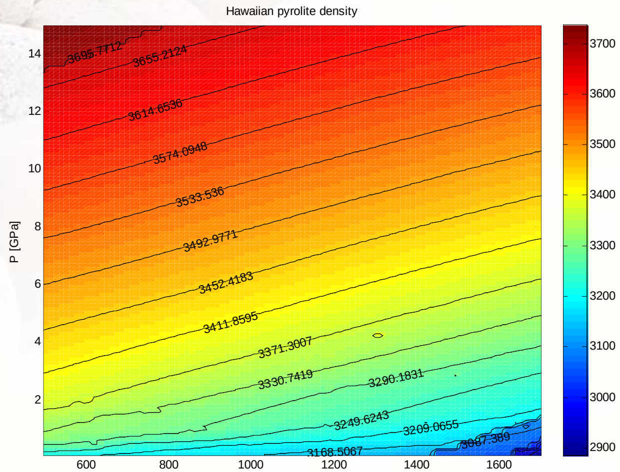

Nina Simon, PGP 2007

Continental lithosphere densities

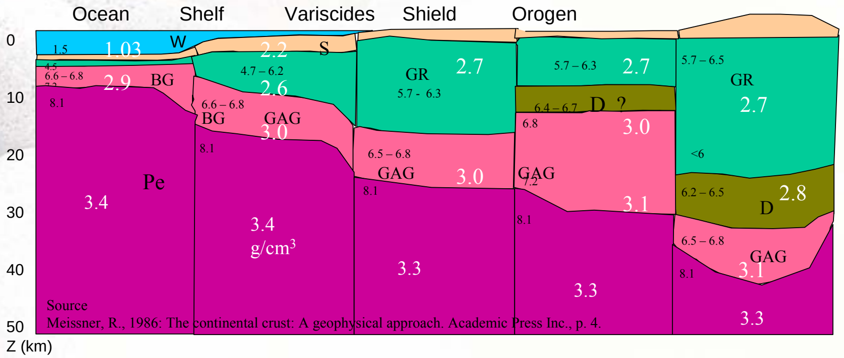

Rock types:

BG = basaltic, gabbroic in oceanic crust
GAG = amphibolitic & granulitic in continental crust
PE = peridotitic, ultramafic
D = Dioritic (?), possibly amphibolitic
S = sediments
GR = granitc gneissic upper crust
W = water

P-wave velocities (km/s):
black numbers

Densities (g/cm^3):
White numbers

Density vs. velocity

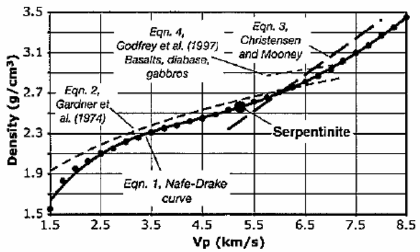

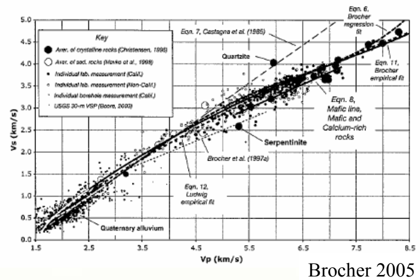

Brocher 2005

Density ρ and velocity have in isotrope, elastic media simple relations:

$$V_P = \sqrt{\frac{\kappa + \frac{4}{3}\mu}{\rho}} = \sqrt{\frac{E(1-\upsilon)}{\rho(1+\upsilon)(1-2\upsilon)}}$$

$$V_S = \sqrt{\frac{\mu}{\rho}} = \sqrt{\frac{E}{2\rho(1+\upsilon)}}$$

κ: compressibility modus
μ: shear (rigidity) modus
E: elasticity module
ν: Poisson ratio

…but Earth is not as simple!

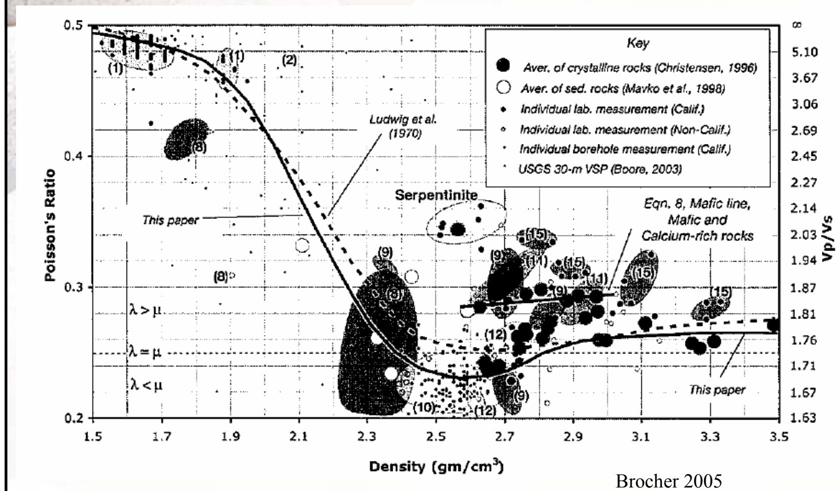

Brocher 2005

Relating density to P-wave velocity

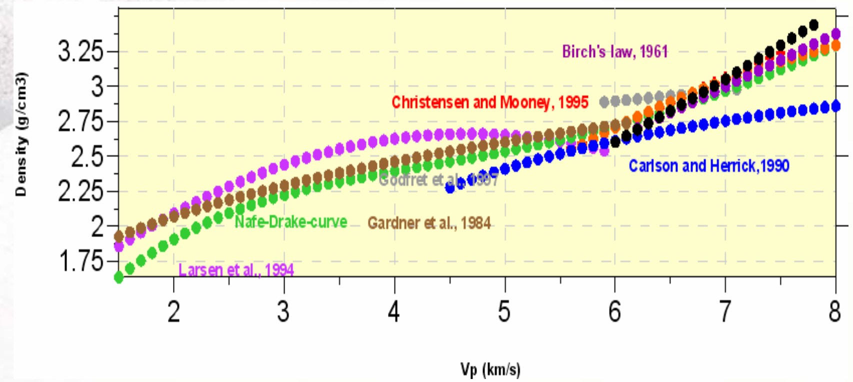

compiled by Laura Marello

Vp-Rho function	Rock type	Velocity range	Remarks
Nafe-Drake (Ludwig et al. 1970)	sedimentary and crystalline rocks	Vp=1.5-8.8 km/s	
Gardner's rule (Gardner et al., 1984)	sedimentary rock	Vp= 1.5-6.1 km/s	
Godfrey et al. 1997	basalts, diabase & gabbros	Vp=5.9-7.1 km/s	
Christensen & Mooney 1995	crystalline rocks	Vp=5.5-7.5 km/s	
Hamilton's relation (Larsen et al. 1994)	empirical relation from 152 sediment cores (ODP) used for shale		
Carlson and Herrick 1990	continent-ocean transition zone and oceanic regions		High velocity gradient in the upper crust
Birch's law 1961	diabase, gabbro, eclogite		
Sobolev-Babeyko 1995	crystalline crust	Vp= 6.05-7.8 km/s	pressure and temperature dependent

compiled by Laura Marello

v_p-ρ-conversion after Sobolev-Babeyko

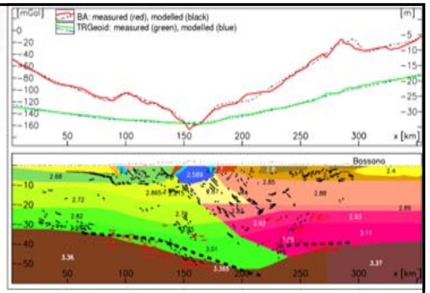

Three steps

1. In situ Velocity to normal velocity

$$\mathbf{v_{p_0}} = \mathbf{v_{p(in\_situ)}} - \frac{\partial \mathbf{v_p}}{\partial \mathbf{P}}\mathbf{P} - \frac{\partial \mathbf{v_p}}{\partial \mathbf{T}}(\mathbf{T}-\mathbf{T_o})$$

with $\partial v_p / \partial P = 0.12 km / sGPA$ and $\partial v_p / \partial T = -4.5 \cdot 10^{-4} km / s°C$

2. Density at normal conditions P_0, T_0.

$\rho_0 = 0.446 \cdot v_{p_o} - 0.074$ for $6.05 km / s \le v_{p_o} \le 6.95 km / s$

$\rho_0 = 0.487 \cdot v_{p_o} - 0.359$ for $6.95 km / s \le v_{p_o} \le 7.80 km / s$

3. Normal density to in situ density

$$\rho_{(in\_situ)} = \rho_0 + \frac{\partial \rho}{\partial P}P + \frac{\partial \rho}{\partial T}(T - T_0)$$

with $\partial \rho / \partial P = 0.05 g / cm^3 GPa$ and $\partial \rho / \partial T = -9 \cdot 10^{-2} kg / m^3 °C$

Relating density to P-wave velocity: an example from TRANSALP

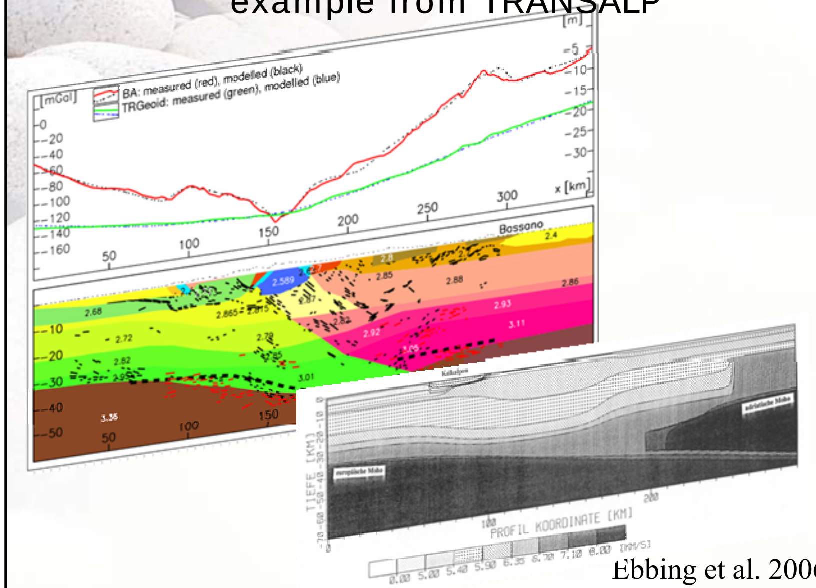

Ebbing et al. 2006

Relating density to P-wave velocity: Sedimentary rocks

For sedimentary rocks different authors have developed empirical relations between density and velocity. Some of these relations are lithology-specific, and the constants in the require adjustments as a of the percentage of sand, shale, and limestone present.

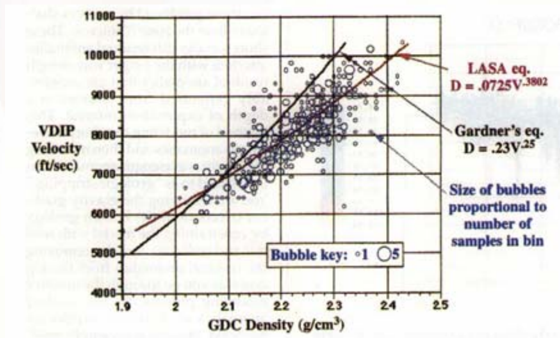

FROM HUSTON ET AL., 1992

DENSITY AS A FUNCTION OF DEPTH
Density driven by compaction, not lithology

Due to the depositional environment and tectonic history of the Gulf of Mexico (and other similar basins), rock densities of the sedimentary section have been found to vary primarily as a function of burial depth. This density-depth relationship is attributed to the very thick (~6000m) pile of clastic sediments that comprise the the Gulf basin onshore and offshore. This density-depth relationships have been extensivly used to model gravity anomalies and to identify salt structures in the subsurface.

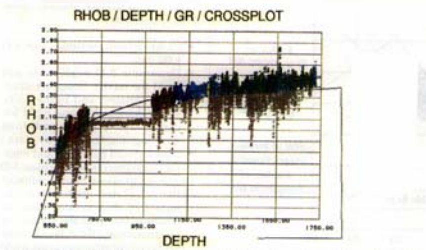

Figure 4. Crossplot of depth versus density showing extrapolation of curve through salt and scatter.

DENSITY VS. DEPTH CROSSPLOT FOR OFFSHORE GULF OF MEXICO STUDY AREA. NOTE THE PRESENCE OF SALT AT 750 TO 1000 METERS DEPTH.

Porosity= pore volume / bulk volume

Density= bulk density * (1-porosity)

For normally pressured sediments, the variation of porosity ϕ with depth y is given by

$$\phi = \phi_0 e^{-cy} \qquad (9.16)$$

where c is a coefficient determining the slope of the ϕ-depth curve, y is the depth, and ϕ_0 is the porosity at the surface. In other words, the surface porosity declines to $1/e$ of its original surface value at a depth of $1/c$ km (Fig. 9.2). On a depth versus log porosity graph, the value of c is the inverse of the rate of change of porosity with depth. The coefficient c can therefore be estimated if a number of porosity measurements can be made, for example from a sonic log from a representative borehole in the basin. This relationship has been applied to a range of different lithologies, each with its own value of c (Sclater and Christie 1980; Halley and Schmoker 1983) (Table 9.1) (Fig. 9.3).

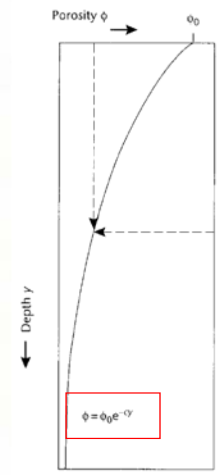

From: Allen, P.A. and Allen, J.R., 2005.Basin Analysis: Principles and Applications, 2. ed.,Blackwell Publishing, 549 pp.

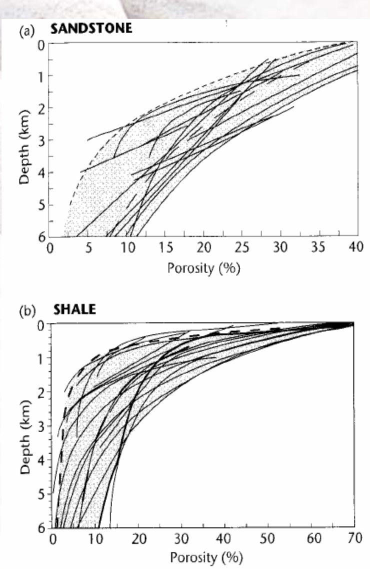

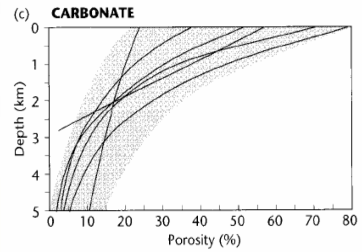

Fig. 9.3 Compilation of porosity–depth curves for sandstones (a), shales (b), and carbonates (c). Sources of datasets in Giles (1997). Note that shales compact early compared to sandstones. The porosity–depth relation for carbonates varies according to grain types and amount of cementation. Reproduced courtesy of Springer.

Giles, M.R., 1997. Diagenesis: A quantitative perspective. For basin modeling and rock property prediction. Kluwer academic Publisher, Dordrecht. Copied from Allen, P.A. and Allen, J.R., 2005. Basin Analysis: Principles and Applications, 2. ed.,Blackwell Publishing, 549 pp.

In ***LithoFlex*** (after Braitenberg et al. 2006, Wienecke 2006):

$$\rho(d) = \Phi_0 \cdot e^{-b \cdot z} \cdot \rho_f + (1 - \Phi_0 \cdot e^{-b \cdot z}) \cdot \rho_S$$

Thereby is **z** the depth and Φ_0 the initial **[Porosity]** of the sediments at the surface. The bulk density of a rock is composed of the **[Fluid density]** ρ_f and the **[Grain/Rock density]** ρ_s related to the porosity of the sediments.

$$\rho_{\exp} = 1.03 \cdot 0.65 \cdot e^{-0.0009d} + 2.67 \cdot (1 - 0.65 \cdot e^{-0.0009d})$$

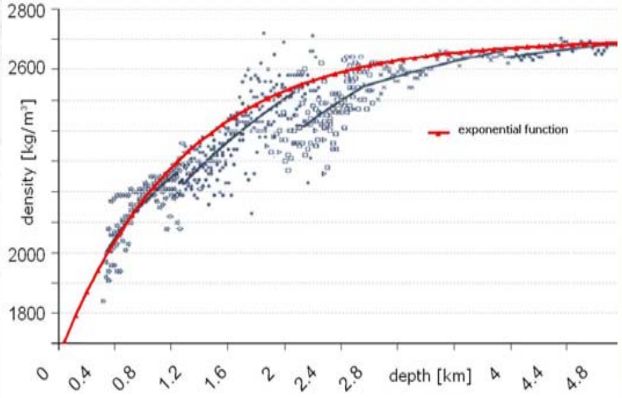

Exponential density function to fit the borehole measurements in the Barents Sea. Tsikalas (1992) compiled all available measured density values and used a linear relation ship to describe the density increase with depth.

Sensitivity to density

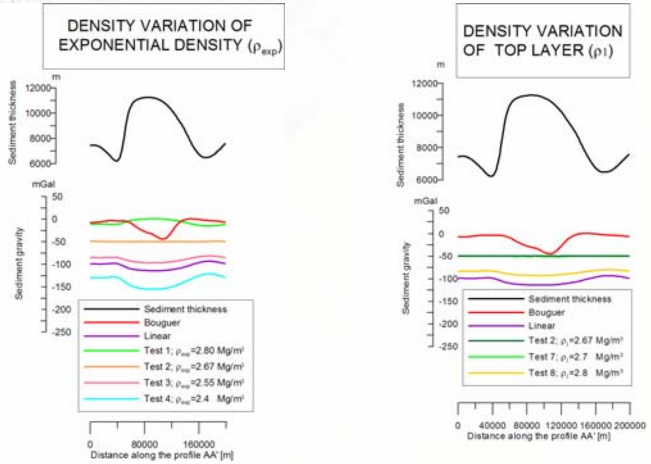

Questions, comments, remarks?

Literature 1/2

Allen, P.A. and Allen, J.R., 2005.Basin Analysis: Principles and Applications, 2. ed.,Blackwell Publishing, 549 pp.

Birch F. (1991). The velocity of compressional waves in rocks to 10 kbar. Part 2', J. Geophys. Res. 66, 2199-2224.

Braitenberg, C., Wienecke, S. and Wang, Y., 2006. Basement structures from Satellite Derived Gravity Field: the South China Sea Ridge. Journal of Geophysical Research-Solid Earth, 111, B05407.

Brocher, T. M. 2005 Empirical Relations between Elastic Wavespeeds and Density in the Earth's Crust Bulletin of the Seismological Society of America; December 2005; v. 95; no. 6; p. 2081-2092

Bungum, H., Ritzmann, O., Maercklin, N., Faleide, J., Mooney, W.D. & Detweiler, S.T. 2005: Three-Dimensional Model for the Crust and Upper Mantle in the Barents Sea Region. *EOS,* 86(16), doi: 10.1029/2005EO160003.

Carlson R.L. and Herrick C.N. (1990).Densities and porosities in the oceanic crust and their variations with depth and age, J. Geophys.Res., 95,9153-9170.

Carmichael, R,S. 1984. Handbook of physical properties of rocks. Volume I (1986), II (1982), III (1984).

Christensen, N. I., and W. D. Mooney (1995). Seismic velocity structure and composition of the continental crust: A global view, J. Geophys. Res. 100, 9761-9788.

Dehls, J.F., Olesen, O., Bungum, H., Hicks, E., Lindholm, C.D. & Riis, F. 2000: Neotectonic map, Norway and adjacent areas 1:3 mill. Norges geologiske undersøkelse, Trondheim, Norway.

Ebbing, J., 2002. 3D-Dichtemodellierung und isostatisches Verhalten der Lithosphäre in den Ostalpen (The 3D density structure and isostatic compensation of the lithosphere in the Eastern Alps). German *Ph.D thesis*, Freie Universität Berlin.

Ebbing, J., 2007: Isostatic density modelling explains the missing root of the Scandes. *Norwegian Journal of Geology,* 87, 13-20.

Ebbing, J., Braitenberg, C. and Götze, H.-J., 2006. The lithospheric density structure of the Eastern Alps. *Tectonophysics,* 414, 145-155.

Ebbing, J., Braitenberg, C. and Wienecke, S., 2007. Insights into the lithospheric structure and the tectonic setting of the Barents Sea region from isostatic considerations. *Geophysical Journal International*, 171 (3), 1390–1403.

Ebbing, J., Skilbrei, J.R. and Olesen, O. 2007. Insights into the magmatic architecture of the Oslo Graben by petrophysically constrained analysis of the gravity and magnetic field, *J. Geophys. Res.*, 112, B04404, doi:10.1029/2006JB004694.

Ebbing J., Olesen, O., Gernigon, L., Reynisson, R.F., og sokkelgeofysikk lag på NGU 2008: Tyngde og magnetiske data viser sporene av gamle strukturer på norsk sokkel. I: Geologi for samfunnet i 150 år –arven etter Kjerulf (T. Slagstad & R. Dahl, eds.), *Gråsteinen* 12, 89-98.

Ebbing, J., Gernigon, L., Pascal, C., Olesen, O. and Osmundsen, P.T., A discussion of structural and thermal control of magnetic anomalies on the mid-Norwegian margin. *Geophysical Prospecting, in press.*

Faleide, J.I., Ritzmann, O., C. Weidle, C. & A. Levshin, A. 2006: Geodynamical aspects of a new 3D geophysical model of the greater Barents Sea region – Linking sedimentary basins to the upper mantle structure. *Geophysical Research Abstracts*, 8, 08640.

Gardner, G. H. F., L. W. Gardner, and A. R. Gregory (1984). Formation velocity and density -The diagnostic basics for stratigraphic traps, Geophysics 39, 770-780.

Godfrey, N. J., B. C. Beaudoin, S. L. Klemperer, and the Mendocino Working Group USA(1997). Ophiolitic basement to the Great Valley forearc basin, California, from seismic and gravity data: Implications for crustal growth at the North American continental margin, Geol.Soc. Am. Bull. 109, 1536-1562.

Karner, G.D., Studinger, M., Bell. R.E., 2005. Gravity anomalies of sedimentary basins and their mechanical implications: Application to the Ross Sea West Antarctica. Earth and Planetary Science Letters, 235(3-4), 577-596.

Literature 2/2

Kinck, J.J., Husebye, E.S. & Larsson, F.R. 1993: The Moho depth distribution in Fennoscandia and the regional tectonic evolution from Archean to Permian times. *Precambrian Research* 64, 23-51.

Korhonen, J.,V., Aaro, S., All, T., Elo, S., Haller, L.Å., Kääriäinen, J., Kulinich, A., Skilbrei, J.R., Solheim, D., Säävuori, H., Vaher, R., Zhdanova, L. & Koistinen, T. 2002a. Bouguer anomaly map of the Fennoscandian shield 1: 2 000 000. Geological Surveys of Finland, Norway and Sweden and Ministry of Natural Resources of Russian Federation.

Kusznir, N.J., Hunsdale, R. and Roberts, A.M., 2004. Timing of depth-dependent lithosphere stretching on the S.Lofoten riftedmargin offshoremid-Norway: pre-breakup or post-breakup?, Basin Research 16, 279–296.

Larsen, H.C., Saunders A.D., Clift P.C., and the Shipboard Scientific Party (1994). Proceeding of the Drilling Program Initial Report. Vol. 152, Ocean Drill. Program. College Station, Tex.

Ludwig W.J., Nafe J.E. and Drake C.L. (1970). Seismic refraction, in the Sea, A.E.Maxwell (Editor), Vol.4, Wiley-Interscience, New York, 52-84

Meissner, R., 1986: The continental crust: A geophysical approach. Academic Press Inc., p. 4

Mjelde, R., Raum, T., Breivik. A., Shimamura, H., Murai, Y., Takanami, T. & Faleide, J.I. 2005: Crustal structure of the Vøring margin, NE Atlantic: a review of geological implications based on recent OBS-data. In: Doré, A.G. & Vining, B.A. (eds.) Petroleum Geology: North-West Europe and Global Perspectives. Proceedings of the 6th Petroleum Geology Conference. Geological Society Special Publication, Geological Society, London, 803-813.

Mjelde, R., Faleide, J.I., Breivik, A.J., Raum, T., Lower crustal composition and crustal lineaments on the Vøring Margin, NE Atlantic: A review, *Tectonophysics* (2008), doi: 10.1016/j.tecto.2008.04.018.

Mussett, A. E., Khan, M.A., 2000. Looking into the earth. An introduction to Geological Geophysics. Cambridge University Press

Olesen, O., Lundin, E., Nordgulen, Ø., Osmundsen, P.T., Skilbrei, J.R., Smethurst, M.A., Solli, A., Bugge, T. & Fichler, C. 2002: Bridging the gap between the onshore and offshore geology in Nordland, northern Norway. *Norwegian Journal of Geology* 82, 243-262.

Olesen, O., Dehls, J.F., Ebbing, J., Kihle, O. & Lundin, E., 2007. Aeromagnetic mapping of deep-weathered fracture zones in the Oslo Region – a new tool for improved planning of tunnels. *Norwegian Journal of Geology*, 87, 253-267.

Ritzmann, O., Maercklin, N., Faleide, J.I., Bungum, Mooney, W.D. & Detweiler, S.T. 2007: A three-dimensional geophysical model of the crust in the Barents Sea region: model construction and basement characterization. *Geophys. J. Int.* 170, 417–435.

Roberts, A.M., Lundin, E. and Kusznir, N.J. 1997. Subsidence of the Vøring Basin and the influence of the Atlantic continental margin. *Journal of the Geological Society*, *London*, 154, 1997, 551–557,

Skilbrei, J.R., Kihle, O., Olesen, O., Gellein, J., Sindre, A., Solheim, D. & Nyland, B., 2000: Gravity anomaly map Norway and adjacent ocean areas, scale 1:3 Million, Geological Survey of Norway, Trondheim.

Sobolev, S. and Babeyko, A., 1994. Modeling of mineralogical composition, density and elastic wave velocities in anhydrous magmatic rocks. Surveys in Geophysics, 15: 515-544.

Tsikalas, F., 1992: *A study of seismic velocity, density and porosity in Barents Sea wells (N. Norway)*. Master Thesis, Department of Geology, University of Oslo, Norway.

Wienecke, S., 2006. A new analytical solution for the calculation of flexural rigidity: significance and applications. PhD Thesis, Free University Berlin, Germany. http://www.diss.fu-berlin.de/2006/42/indexe.html.

Wienecke, S., Ebbing, J. & Gernigon, L. 2007: 3D density modelling, isostasy and elastic thickness calculation of the Barents Sea. NGU Report 2007.022. 56pp.